UC Irvine
UC Irvine Previously Published Works

Title
Fast-ion D-alpha diagnostic for NSTX

Permalink
https://escholarship.org/uc/item/94w2f40d

Journal
Review of Scientific Instruments, 77(10)

ISSN
0034-6748

Authors
Heidbrink, WW
Bell, RE
Luo, Y
et al.

Publication Date
2006-10-01

DOI
10.1063/1.2221902

Copyright Information
This work is made available under the terms of a Creative Commons Attribution License, availalbe at https://creativecommons.org/licenses/by/4.0/

Peer reviewed

eScholarship.org Powered by the California Digital Library
University of California

Fast-ion *D*-alpha diagnostic for NSTX

W. W. Heidbrink
University of California, Irvine, Irvine, California 92697

R. E. Bell
Princeton Plasma Physics Laboratory, Princeton University, Princeton, New Jersey 08543

Y. Luo
University of California, Irvine, Irvine, California 92697

W. Solomon
Princeton Plasma Physics Laboratory, Princeton University, Princeton, New Jersey 08543

(Received 10 May 2006; presented on 10 May 2006; accepted 2 June 2006; published online 9 October 2006)

A fast-ion *D*-alpha (FIDA) diagnostic is under development for the National Spherical Torus Experiment (NSTX). The FIDA technique is a charge-exchange recombination spectroscopy measurement that exploits the large Doppler shift of Balmer-alpha light from energetic hydrogenic atoms to infer the fast-ion density. The principal objective of the NSTX installation is to measure the transport of beam ions caused by fast-ion driven instabilities; detection of perpendicular acceleration of fast ions during high harmonic fast wave heating is another important goal. Recent data from a DIII-D FIDA diagnostic guide the design. The planned NSTX diagnostic consists of two separate instruments focusing on different aspects of the measurement. One instrument uses a transmission grating spectrometer to measure the perpendicular energy spectrum and the spatial profile every 10 ms; the anticipated resolution is ~10 keV in energy and ~5 cm in radius. A second instrument employs bandpass filters to detect fast-ion redistribution events with millisecond temporal resolution. © *2006 American Institute of Physics.* [DOI: 10.1063/1.2221902]

I. INTRODUCTION

The diagnosis of fast ions is an important element of the National Spherical Torus Experiment (NSTX) program. The main auxiliary heating systems on NSTX are the neutral beams and the high harmonic fast wave (HHFW) system. Transport studies of energy, current, momentum, and particle confinement require accurate knowledge of the fast-ion profile. Since fast-ion driven instabilities occur in nearly every beam-heated NSTX discharge,[1] deviations from neoclassical fast-ion confinement are a virtual certainty. The HHFW system is another vital tool. Because wave absorption by fast ions[2] competes with electron absorption, it can severely impact electron heating and current drive by the fast waves.

The ideal fast-ion diagnostic would measure the entire distribution function in space, velocity, and time, $f_f(\mathbf{r},E,v_\parallel/v,t)$. (Here E is the energy and $v_\parallel/v$ is the pitch of the velocity vector relative to the magnetic field.) The fast-ion *D*-alpha (FIDA) concept[3] measures light emitted by fast ions that neutralize when they pass through a heating beam. Fast neutrals that are in an excited state can emit the Balmer-alpha line, which is the transition from the $n=3$ to the $n=2$ energy level. This D_α transition emits a visible photon, which is easily measured using standard optical fibers, lenses, spectrometers, and cameras. Conceptually, the use of D_α light to diagnose a fast deuterium population is similar to the diagnosis of fast helium populations using charge-exchange recombination (CER) spectroscopy.[4,5] The D_α signal from fast ions was first detected in DIII-D using a CER spectrometer that was tuned to the blue side of the D_α line.[3] During the 2005 campaign on DIII-D, a dedicated instrument[6] that measured the full spectrum collected data. In addition, on selected discharges, a spatial array of vertically viewing fibers measured a portion of the spectrum. These instruments established FIDA spectroscopy as a powerful new technique for the diagnosis of f_f. The DIII-D data demonstrate energy resolution of ~10 keV, temporal resolution of ~1 ms, and are consistent with a spatial resolution of ~5 cm.[7] This article describes the design criteria and plans for a FIDA diagnostic on NSTX.

II. DESIGN CRITERIA FOR THE NSTX DIAGNOSTIC

Since the DIII-D results demonstrate the feasibility of the D_α technique, we discuss the NSTX design relative to DIII-D.

Viewing angle. The Doppler shift of an emitted photon is proportional to the velocity component of the radiating neutral along the line of sight. An analogous situation occurs for fast-ion diagnosis with collective Thomson scattering, which also measures a single component of the velocity vector. Egedal and Bindslev[8] studied mathematically the relationship between velocity-component measurements and "gyrotropic" velocity-space distributions. (A gyrotropic distribution function only depends on two velocity components because of rapid gyromotion.) They find that, although it is not possible to uniquely reconstruct $f_f(E,v_\parallel/v)$ from the one-dimensional velocity measurements, a reasonable reconstruc-

 © 2006 American Institute of Physics

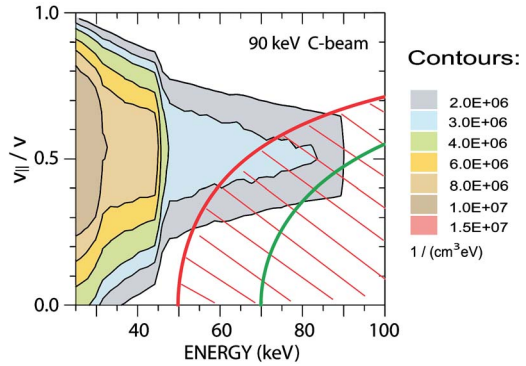

FIG. 1. Fast-ion distribution (averaged over the volume) in a NSTX discharge during injection of the most perpendicular source (source C) at 90 keV as calculated by TRANSP (Ref. 13). The steps at 30 and 45 keV are associated with the third- and half-energy components. The distribution is relatively narrow because pitch-angle scattering is weak. The red line and the hatched region indicate the portion of the distribution function that contributes to the spectral intensity at the wavelength that corresponds to 50 keV; similarly, the wavelength that corresponds to 70 keV measures ions to the right of the green line.

tion can be obtained with two aptly chosen views.

For a FIDA diagnostic, additional practical considerations are also important. The most significant of these is the bright interference from other neutrals. This light is most easily avoided with a viewing angle that is perpendicular to the injected neutral beam.[3] For NSTX, the neutral beams are injected horizontally, so a vertical view satisfies this requirement. Another complication is that the charge-exchange probability depends on the relative velocity between the injected neutrals and the fast ions but a vertical view also tends to minimize the sensitivity to these effects.[3]

Two additional considerations in charge-exchange spectroscopy of impurity ions are the "plume" formed by ions that stream along field lines[9] and distortions of the spectrum associated with the finite lifetime of the excited state of the gyrating ions.[10] Since hydrogen ions become neutral atoms in a charge-exchange event, they travel in straight lines and are immune to these complications. Thus, in contrast to impurity-ion measurements of poloidal rotation, there is no obvious benefit in having paired upward and downward vertical views.

Spectral range. The basic features of the fast-ion distribution function (Fig. 1) are very similar in the two devices. DIII-D injects deuterium neutrals up to 81 keV; the maximum energy in NSTX is 110 keV. The angles of injection are similar. Because the electron temperature is typically lower in NSTX, fast ions slow down predominately on electrons and pitch-angle scattering is less important than in DIII-D. This implies that the maximum perpendicular energy during beam injection is very similar in the two devices. In both devices, rf heating can accelerate a tail above the injection energy but few fast ions have perpendicular energies in excess of ~120 keV. Thus, the spectral range of the NSTX instrument should be similar to that of the DIII-D spectrometer, i.e., approximately 15 nm.

Spectral resolution. Theoretically, even in the presence of instabilities, the fast-ion distribution function does not have particularly sharp features in velocity space. Experimentally, the technique performs an effective average over the relevant velocity-space variables (Fig. 1) and Stark splitting smears the line an additional ~1 nm. Thus, as far as diagnosis of f_f, spectral resolution as poor as 0.5 nm is adequate. In practice, somewhat better resolution is desirable to detect contamination of the spectrum by impurity lines but the requirements are still modest. Use of a wide entrance slit to maximize signal levels is appropriate.

Bright interference and dynamic range. The unshifted light from edge and injected neutrals is brighter by several orders of magnitude than the desired fast-ion signal. In the DIII-D installation, a bar was inserted in the focal plane of the spectrometer to block the unshifted light.[6] Some light from warm thermal (halo) neutrals extended beyond the blocking bar but these signal levels did not saturate the charge-coupled device (CCD) camera. The halo intensity, which is proportional to the neutral beam deposition rate, is comparable in NSTX and DIII-D. Moreover, because the ion temperature tends to be lower in NSTX than in DIII-D, the width of the thermal (halo) line is narrower, making it even easier to block the bright D_α light from other sources with a blocking bar or alternative technique.

Impurity contamination and visible bremsstrahlung. The dominant impurities are the same in NSTX and DIII-D: carbon, oxygen, and boron. In the future, lithium may become important in NSTX but lithium does not have a strong transition in the spectral region of interest. Since the densities are similar, the visible bremsstrahlung backgrounds are similar. Beam modulation techniques were employed in DIII-D to remove backgrounds. This effectively eliminated all impurity lines except for two weak charge-exchange recombination lines associated with boron and carbon. Since fewer neutral beam injectors are available at NSTX, beam modulation is not feasible for most experiments. In NSTX, toroidally displaced fiber views that miss the injected heating beam are employed for background subtraction.

Edge localized modes (ELMs). Both DIII-D and NSTX experience periodic ELMs during *H*-mode operation that cause large, transient changes in edge D_α and impurity emission. In the DIII-D installation, background levels changed during ELMs, presumably due to unshifted D_α light that scatters in the spectrometer. The use of a blocking bar made it impossible to monitor the unshifted intensity simultaneously, however. In NSTX, it is desirable to pass ~0.1% of the unshifted D_α light as a monitor of its intensity. This could be accomplished with a suitable notch filter if one is available. Alternatively, the opaque blocking bar could be replaced by a neutral-density filter strip in the focal plane. If a blocking bar is employed, it will be coated with highly absorbent gold black to minimize spectral contamination by reflected light.

Spatial resolution. The cross-sectional area of NSTX is nearly identical to that of DIII-D. Because 80 keV deuterium neutrals in the $n=3$ energy state travel a mean free path of ~5 cm before undergoing the $3\rightarrow 2$ radiative transition, the spatial resolution of the diagnostic cannot be better than ~5 cm. For typical densities, the injected neutral beam becomes weak ~20 cm past the magnetic axis of the device. Thus, the optimal spatial array for a fast-ion D_α instrument in

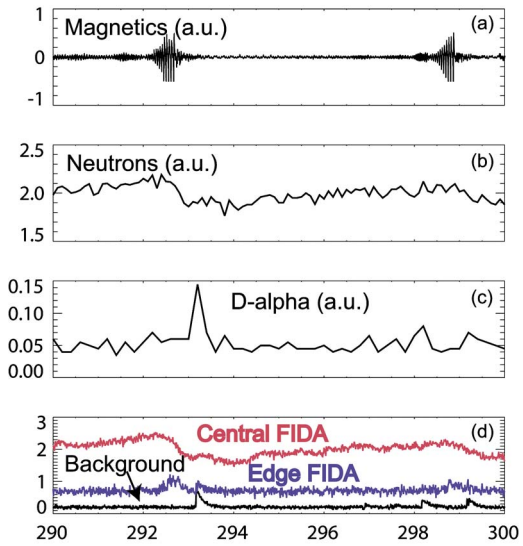

FIG. 2. Time evolution of (a) a $\dot{B}$ signal, (b) the signal from a neutron scintillator, and (c) cold D_α light for a discharge with strong $n=1$ "fishbone" activity with frequencies between 10 and 25 kHz in NSTX. (d) Fake data from three channels of the planned fast system. A central channel detects the loss of fast ions from the core, an edge channel detects redistribution to the outer portion of the plasma, and a background signal monitors changes associated with edge neutrals and impurities.

NSTX consists of a radial array separated by ~5 cm that spans from the outer edge past the magnetic axis, i.e., about 16 channels.

Temporal resolution. Fast-ion instabilities on NSTX change rapidly. It is common for one type of activity to occur for only about 10 ms; then another type predominates. Bursts of activity occur frequently. The duration between bursts can be 5–10 ms, as in the example shown in Fig. 2, but often the cycle repeats far more rapidly. These bursts almost certainly alter f_f locally and sometimes alter the total fast-ion population, as indicated by the drop in the neutron signal at 293 ms in Fig. 2(b). At DIII-D, a high quantum efficiency CCD camera with fast readout capability acquired data every millisecond and the signal levels were adequate to detect ~10% changes in the density of fast ions with vertical energy components above 40 keV. Since the fast-ion density is typically smaller in NSTX than in DIII-D, higher throughput optics are desirable in order to detect redistribution events on a millisecond time scale.

III. PLANNED INSTRUMENTS

The ideal system would provide full spectra for 16 spatial chords at 1 ms temporal resolution. This could be achieved with four fast readout CCD cameras each with its own spectrometer but this solution is several times more expensive than the approach discussed here. Our approach is to use two complementary systems. A spectrometer and camera (Fig. 3) measure the spectra and spatial profile with 10 ms time resolution. Another system (Fig. 4) with poor spectral resolution but excellent temporal resolution investigates rapidly changing phenomena.

Ports at bay A extend vertically above and below the heating beams. Light is focused onto an array of 600 μm diameter fibers by a 200 mm, $f/1.8$ lens at this port. A similar installation at bay B also views the plasma vertically but misses the heating beams; these fibers are used for measurements of the background. Collections of fibers from the same radial location increase the collected light in both instruments. (In the spectrometer, they are stacked vertically.)

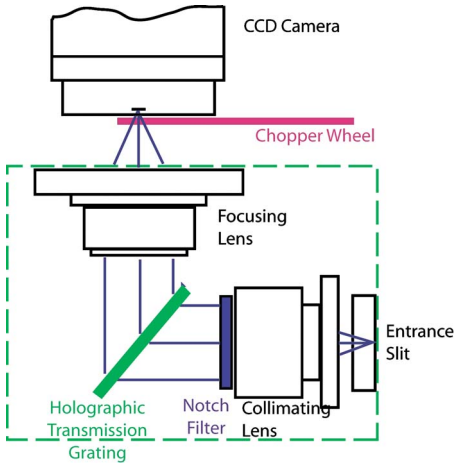

FIG. 3. Schematic of spectrometer and detector. (Adapted from Ref. 14.)

The spectrometer is based on the present NSTX charge-exchange recombination diagnostic[11] (Fig. 3). Because the instrument operates at a fixed wavelength, we can employ a high throughput spectrometer with a transmission grating in lieu of a Czerny-Turner spectrometer. A curved slit holder is required to provide a straight image at the camera.[11] To accommodate all of the spatial channels without cross-talk during CCD readout, a chopper wheel is employed. Spectra are acquired every 10 ms and the light is blocked for 2–3 ms. To block the bright unshifted light, two options are possible. One solution is a notch filter mounted in the spectrometer. The ideal notch filter would transmit a small fraction of the light at 656 nm but would pass light ±1 nm away from the centerline. (We have not found a vendor for such a notch filter yet.) The second option is to place an object at the exit focal plane of the spectrometer, as in the DIII-D design.[6] If this option is pursued, we will try to replace the opaque blocking bar with a partially transmitting neutral-density filter to attenuate but not entirely eliminate the central line. The camera is a high quantum efficiency unit such as the Photonmax 512B.

A bandpass filter is the key element of the fast system (Fig. 4). Since the blue side of the spectrum has fewer impurity lines than the red side, the bandpass filter is centered at 653 nm. A three-cavity filter that is 2 nm wide is well suited to this application. After passing the filter, the light is collected by a high quantum efficiency photodetector. The system accommodates four channels, at least one of which

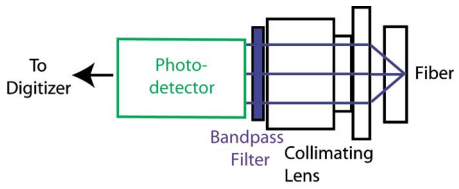

FIG. 4. Schematic of one channel of the fast instrument.

must be devoted to measurement of the background. The radial position of the selected channels varies depending on the instability under study. Radii that correspond to the peak of the instability's spatial eigenfunction are of particular interest.

The anticipated signal levels are sufficient to measure energy spectra with 10 ms resolution with the spectroscopic system and to detect ~10% changes in density with 1 ms resolution with the fast system. Relative to DIII-D, the optical throughput is improved by ~10 (~6 from the f numbers and ~1.8 from the increased efficiency of the spectrometer). Changes in signal and background are more difficult to estimate. The signal level is proportional to the product of fast-ion density and injected neutral density. The injected neutral density of $O(10^8)$ cm^{-3} is very similar in the two devices. The fast-ion density varies greatly for different plasma conditions. When DIII-D is operated at low toroidal field for similarity experiments, the fast-ion density is nearly identical in the two devices;[12] however, in high-performance DIII-D plasmas, the fast-ion density can be an order of magnitude greater than the typical NSTX value of $O(10^{12})$ cm^{-3}. On the other hand, because of the lower temperatures, backgrounds also tend to be weaker in NSTX: bremsstrahlung is about two times smaller and interference from halo (thermal) neutrals becomes negligible.

The spectroscopic system is expected to acquire data in 2007.

ACKNOWLEDGMENTS

The assistance and encouragement of Russ Feder, Emil Ruskov, and Dave Johnson are gratefully acknowledged. This project is supported by the U.S. Department of Energy.

[1] E. D. Fredrickson *et al.*, Phys. Plasmas **10**, 2852 (2003).
[2] A. L. Rosenberg *et al.*, Phys. Plasmas **11**, 2441 (2004).
[3] W. W. Heidbrink, K. H. Burrell, Y. Luo, N. A. Pablant, and E. Ruskov, Plasma Phys. Controlled Fusion **46**, 1855 (2004).
[4] M. G. Von Hellermann, W. G. F. Core, J. Frieling, L. D. Horton, R. W. T. Konig, W. Mandl, and H. P. Summers, Plasma Phys. Controlled Fusion **35**, 799 (1993).
[5] G. McKee *et al.*, Phys. Rev. Lett. **75**, 649 (1995).
[6] Y. Luo, K. H. Burrell, and W. W. Heidbrink, Rev. Sci. Instrum. **75**, 3468 (2004).
[7] Y. Luo, W. W. Heidbrink, K. H. Burrell, P. Gohil, and D. Kaplan, Rev. Sci. Instrum. (submitted).
[8] J. Egedal and H. Bindslev, Phys. Plasmas **11**, 2191 (2004).
[9] R. J. Fonck, D. S. Darrow, and K. P. Jaehnig, Phys. Rev. A **29**, 3288 (1984).
[10] R. E. Bell and E. J. Synakowski, AIP Conf. Proc. **547**, 39 (2000).
[11] R. E. Bell, Rev. Sci. Instrum. **75**, 4158 (2004).
[12] W. W. Heidbrink, E. Fredrickson, N. N. Corelenkov, A. W. Hyatt, G. Kramer, and Y. Luo, Plasma Phys. Controlled Fusion **45**, 983 (2003).
[13] R. V. Budny, Nucl. Fusion **34**, 1247 (1994).
[14] R. E. Bell, L. E. Dudek, B. Grek, D. W. Johnson, and R. W. Palladino, Rev. Sci. Instrum. **70**, 821 (1999).